Supplementary Information - Enhanced Southern Ocean CO_2 outgassing as a result of stronger and poleward shifted southern hemispheric westerlies

L. Menviel[1,2,3*], P. Spence[3,4], A. E. Kiss[5,6], M. A. Chamberlain[4,7], H. Hayashida[4,8], M. H. England[1,3], and D. Waugh[1,3,9]

[1]Climate Change Research Centre, University of New South Wales, Sydney, Australia
[2]Earth and Sustainability Science Research Centre, University of New South Wales, Sydney, Australia
[3]The Australian Centre for Excellence in Antarctic Science, University of Tasmania, Hobart, Tasmania 7001, Australia
[4]Institute for Marine and Antarctic Studies and Australian Antarctic Program Partnership, University of Tasmania, Hobart, Australia
[5]Research School of Earth Sciences, Australian National University, Canberra, Australia
[6]Australian Research Council Centre of Excellence for Climate Extremes, Australia
[7]CSIRO Oceans and Atmosphere, Hobart, Australia
[8]Application Laboratory, Japan Agency for Marine-Earth Science and Technology, Yokohama, Japan
[9]Dpt. of Earth and Planetary Sciences, John Hopkins University, Baltimore, USA

Correspondence: L. Menviel (l.menviel@unsw.edu.au)

Text S1

Changes in oceanic remineralised carbon concentration (C*org*) between 1980 and 2021 are estimated as follows:

$$\Delta Corg = R_{C/P}\Delta PO_{4Reg}, \quad (1)$$

with

$$\Delta PO_{4Reg} = R_{P/O2}\Delta AOU. \quad (2)$$

AOU is the apparent oxygen utilisation, and is the difference between the dissolved oxygen at saturation (as a function of temperature and salinity) and the simulated dissolved oxygen concentration. $R_{C/P}$ and $R_{P/O2}$ are the Redfield ratios equal to 106/1 and 1/172, respectively.

10 **References**

Olsen, A., Key, R. M., van Heuven, S., Lauvset, S. K., Velo, A., Lin, X., Schirnick, C., Kozyr, A., Tanhua, T., Hoppema, M., Jutterstrom, S., Steinfeldt, R., Jeansson, E., Ishii, M., PÃ©rez, F. F., and Suzuki., T.: The Global Ocean Data Analysis Project version 2 (GLODAPv2) - an internally consistent data product for the world ocean, Earth System Science Data, 8, 297–323, 2016.

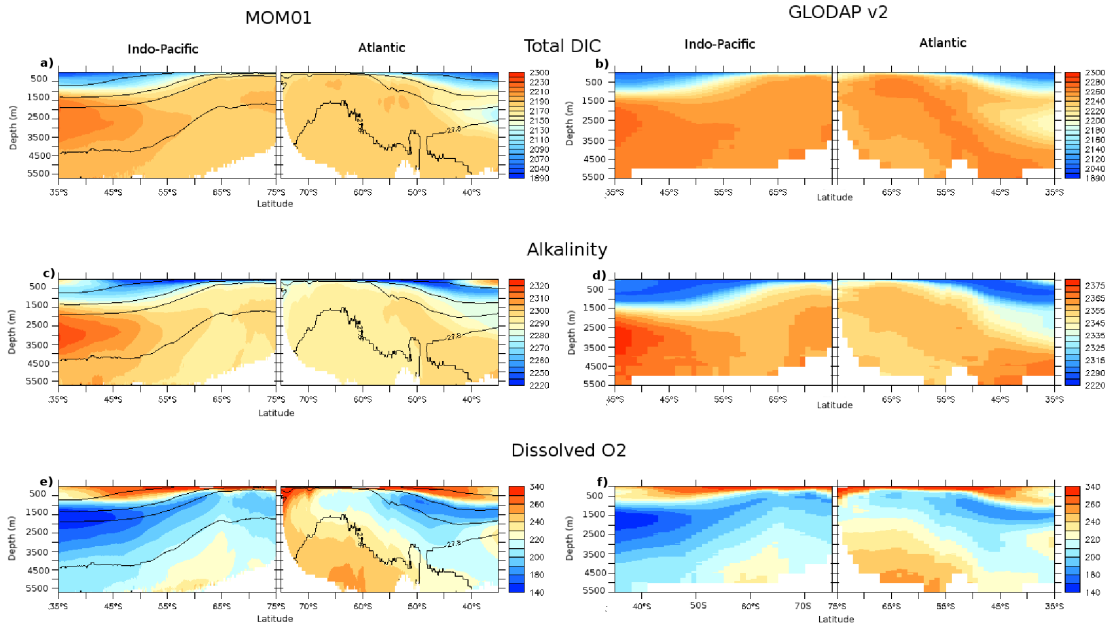

Supplementary Fig. 1. Biogeochemical tracers distribution (left) as simulated in years 1990-2010 in the numerical model and compared to (right) the observed GLODAP v2 dataset (Olsen et al., 2016) for **a,b,** tDIC (μmol kg^{-1}), **c,d,** alkalinity (μmol kg^{-1}), and **e,f,** dissolved oxygen (μmol kg^{-1}), zonally averaged over the Indo-Pacific and Atlantic basins. The density of the AABW ($\geq$1028.31 kg/m^3), the AAIW (1027.5$\leq$AAIW$\leq$1026.95 kg/m^3) and the SAMW ($\leq$1026.95 kg/m^3) are overlaid. The core of PDW (1027.7 kg/m^3) and NADW (1027.75 kg/m^3) are also overlaid in the Indo-Pacific and Atlantic sectors respectively.

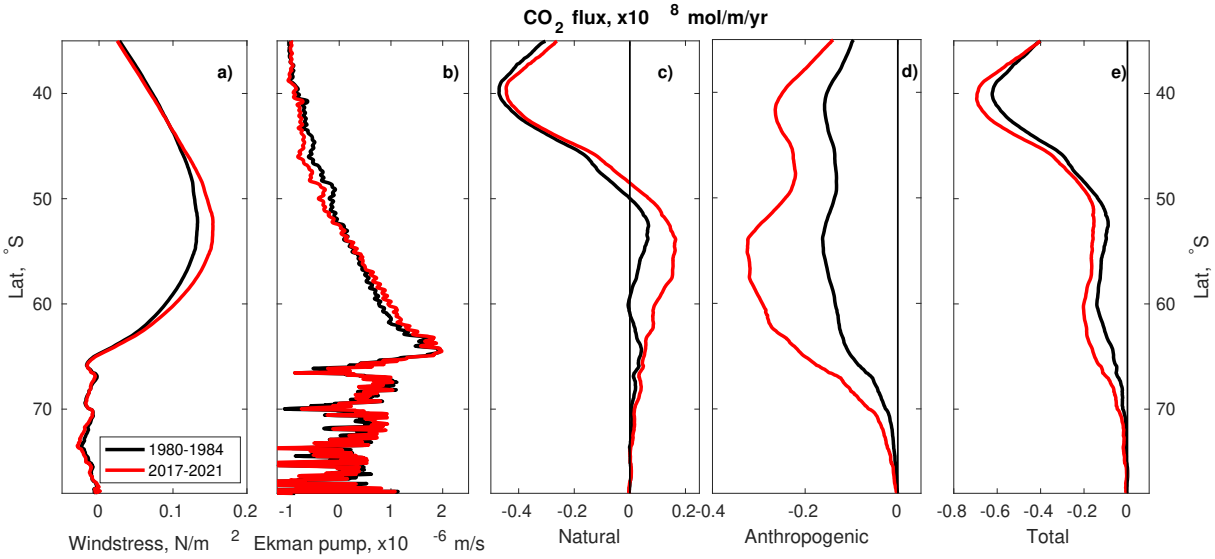

Supplementary Fig. 2. Zonally averaged a) windstress (N/m^2), b) Ekman pumping (m/s), and zonally integrated c) natural, d) anthropogenic and e) total ocean to atmospheric CO_2 flux (mol/m/yr) for years (black) 1980-1984 and (red) 2017-2021 of the numerical experiment.

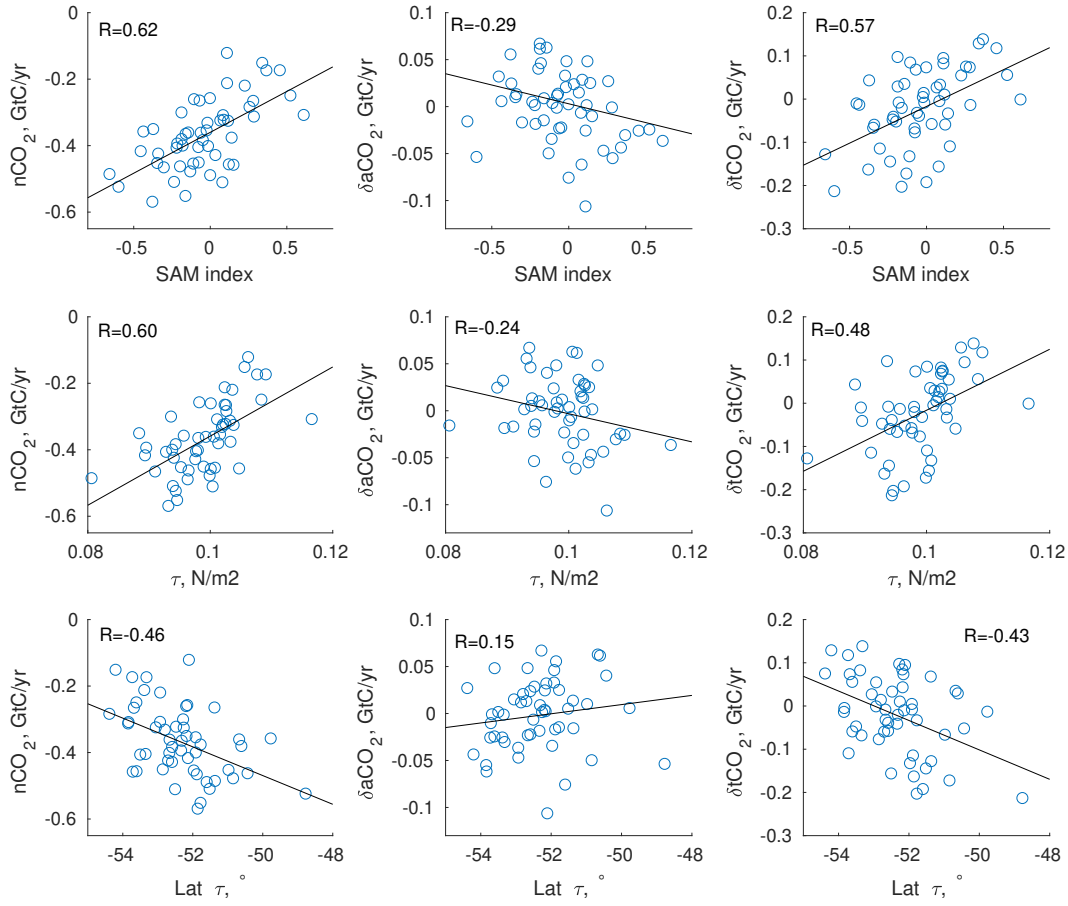

Supplementary Fig. 3. Scatter plots of annual mean SO (left) natural, (middle) detrended anthropogenic and (right) detrended total CO_2 fluxes as a function of annual mean (top) SAM index calculated from JRA55-do dataset, (middle) SO zonal mean windstress, and (bottom) latitude of the maximum windstress. Black lines indicate the linear fit.

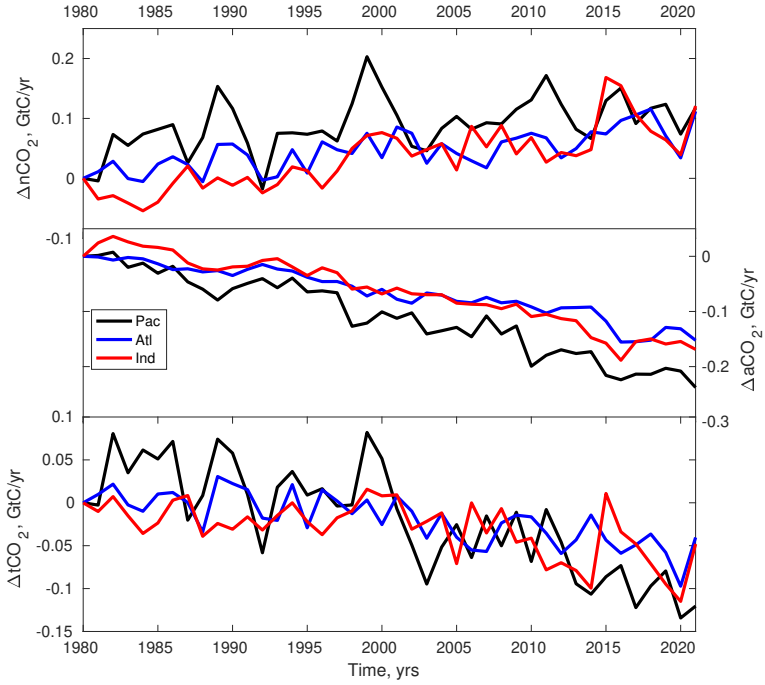

Supplementary Fig. 4. (from top to bottom) nCO_2, aCO_2 and tCO_2 anomalies (GtC/yr) compared to 1980 and integrated over the (blue) Atlantic, (red) Indian and (black) Pacific sectors of the Southern Ocean (south of 35°S).

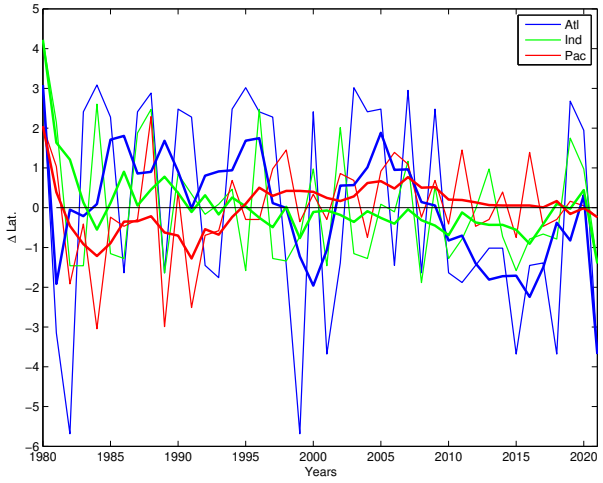

Supplementary Fig. 5. Change in the latitude (°) of the maximum windstress in the (blue) Atlantic, (green) Indian and (red) Pacific sector of the Southern Ocean compared to the 1980-2021 mean. A negative change indicates a poleward shift. The thin lines represent annual mean data, while the thick lines are 5-years running means.

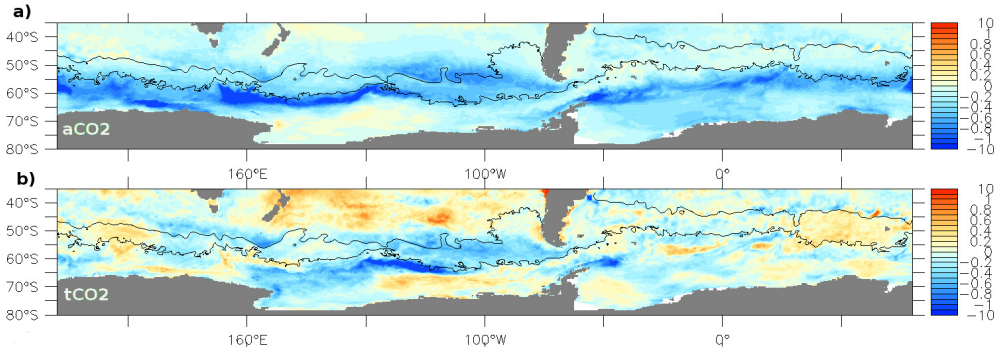

Supplementary Fig. 6. a) aCO_2 and b) tCO_2 flux (mol/m^2/yr) anomalies for a composite of positive phases of the SAM ($\geq$0.83, i.e. 1998, 1999, 2010, 2015 and 2021) compared to a composite of negative SAM years (1980, 1991, 1992, 2002).

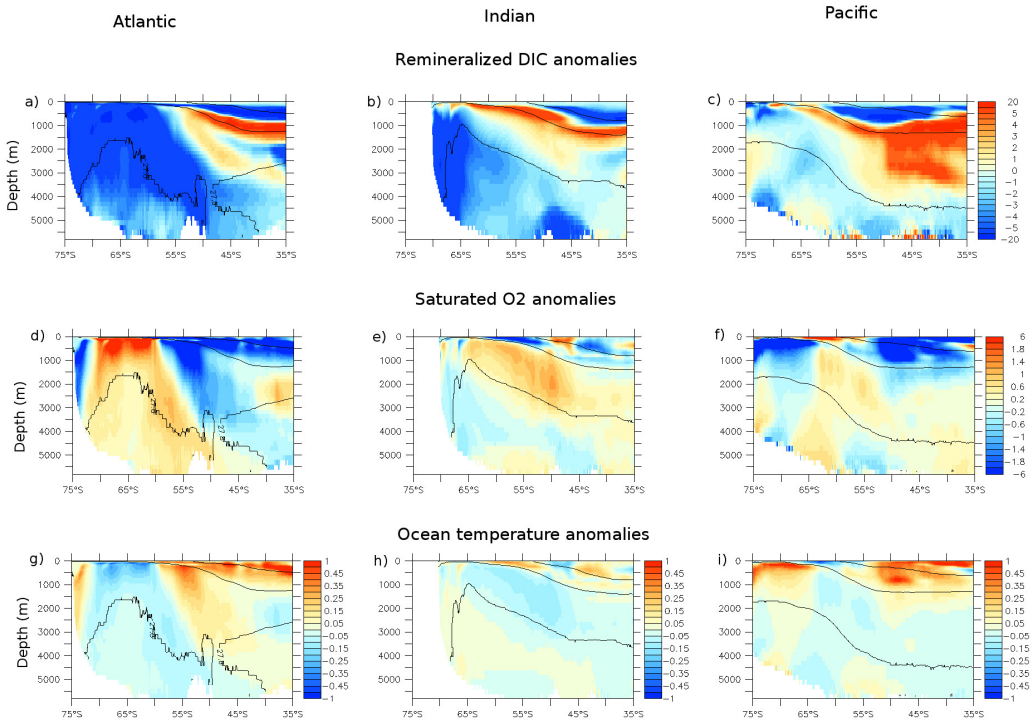

Supplementary Fig. 7. Zonally averaged (a-c) remineralized DIC (mmol/m^3), (d-f) saturated dissolved O_2 (mmol/m^3) and (g-i) ocean temperature ($^\circ$C) anomalies for years 2017-2021 compared to 1980-1982 over the (left) Atlantic, (middle) Indian and (right) Pacific basins.

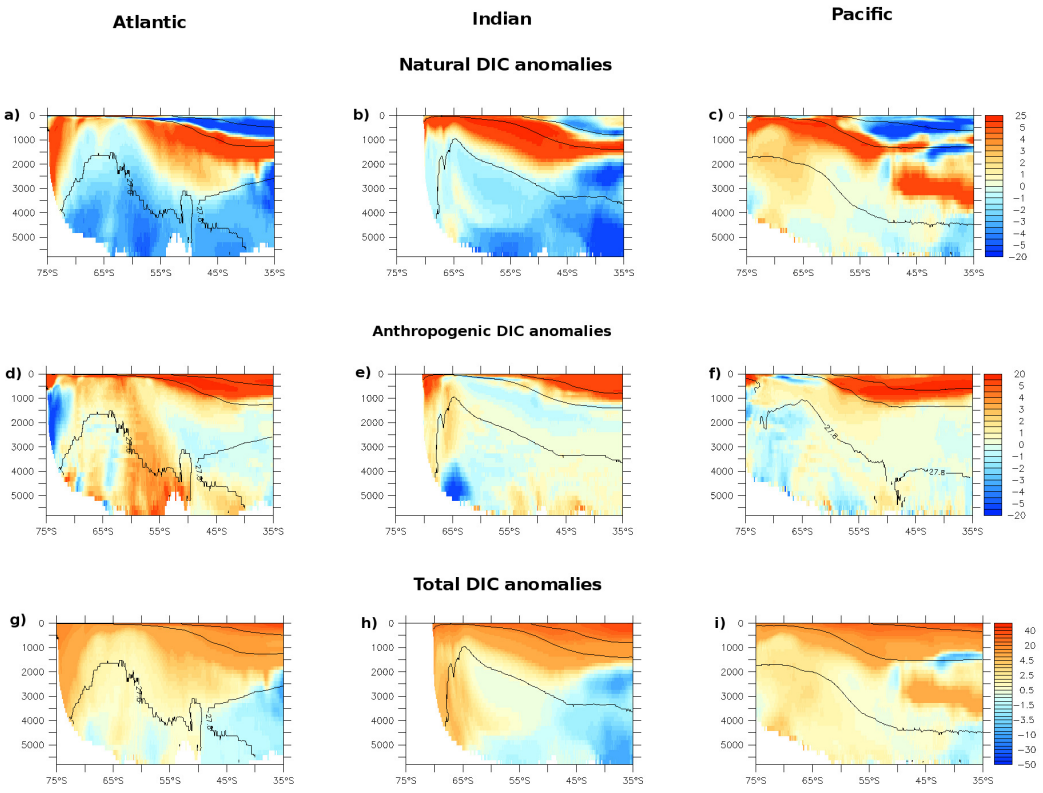

Supplementary Fig. 8. Zonally averaged (a-c) natural DIC, (d-f) anthropogenic DIC and (g-i) total DIC anomalies (mmol/m^3) averaged over (left) the Atlantic, (middle) the Indian and (right) the Pacific for years 2017-2021 compared to 1980-1982. The density of the AABW ($\geq$1028.31 kg/m^3), the AAIW (1027.5$\geq$AAIW$\geq$1026.95 kg/m^3) and the SAMW ($\leq$1026.95 kg/m^3) are overlaid.